Influence of antiferromagnetic spin ordering on the far-infrared active optical phonon modes of α-MnSe

D. M. Djokić* and Z. V. Popović
Centre for Solid State Physics and New Materials, Institute of Physics, Pregrevica 118, 11080 Belgrade, Serbia

F. R. Vukajlović
Institute for Nuclear Sciences-Vinča, P.O. Box 522, 11 001 Belgrade, Serbia

(Received 8 October 2007; published 30 January 2008)

The effects of spin-phonon interaction and magnetic anisotropy on the temperature dependence of the infrared optical phonon modes in the antiferromagnetic α-MnSe are investigated by use of Green's function formalism within $1/z$ perturbation framework. The renormalization effects are calculated explicitly as a function of temperature, phonon-phonon, and spin-phonon interaction constants. Temperature dependence of the renormalized LO phonon frequencies of the F_{1u} infrared active and combinational phonon modes are calculated and compared with experimental data. We have shown that the inclusion of anisotropy is necessary in order to get a good quantitative agreement with the experiment.

DOI: 10.1103/PhysRevB.77.014305 PACS number(s): 63.20.kk, 75.30.Ds, 75.50.Ee, 78.30.Fs

I. INTRODUCTION

Effects of spin ordering on the microscopic and macroscopic dielectric properties are investigated for many magnetic crystals as a function of either temperature or magnetic field.[1–3] In the present theoretical study, the influence of the antiferromagnetic (AF) spin ordering on the observed far-infrared reflectivity spectra of α-MnSe is considered in detail. We apply the usual extension of Heisenberg model which includes the spin-phonon interaction terms and perform a low-density perturbation expansion.[4–6] The recent experimental findings[7] have guided us in that direction. It will be shown that simple noninteracting spin-wave theory is enough to account for the relevant physical properties of α-MnSe in far-infrared spectral region mainly because magnon-magnon interactions do not lead to the two-magnon bound states in this three-dimensional and high-spin AF system. In addition, it also happens that the *pseudodipolar* magnetic anisotropy is of the vital importance for the explanation of measured Raman scattering and infrared spectra.[7,8] The magnetic anisotropy has been taken into account in such a direct way in order to explain mechanical properties of some of the AF semiconductors. Because there is no structural phase transition in this ideal cubic antiferromagnet α-MnSe, no new phonon modes will appear below the magnetic transition temperature. Consequently, only magnetic degrees of freedom are responsible for suitable explanation of the observed spectra. In addition, we have extracted the exchange parameters for the first (J_1) and second (J_2) neighbors by making use of the magnetic susceptibility measurements of α-MnSe.[7]

The hardening of the optical phonon modes is one of the characteristic features of magnetic insulators (mainly antiferromagnets) in the low-temperature ordered phase (cf. Refs. 9 and 10 and references cited therein), but without appropriate microscopic explanation so far. Several earlier attempts were performed on purely phenomenological basis and only with a partial success.[3,9–11] We have shown in this investigation that the spin-phonon interaction, which arises due to a modulation of the exchange interaction by ionic vibrations,[12,13] can describe accurately such a temperature dependence of phonon frequencies. Note also that the occurrence of the mentioned hardening is very typical in systems with pronounced insulating properties, as α-MnSe is, in contrast to those systems exhibiting a metallic behavior.[14]

II. MAGNETIC HAMILTONIAN FOR THE ANTIFERROMAGNETIC α-MnSe

In order to treat the dynamical properties of a type II AF system such as α-MnSe (cf. Fig. 1), characterized by the high-spin value $\frac{5}{2}$ localized on manganese atoms and large number of interacting neighbors, we shall make an approximation which will enable us to use all benefits from representing spin operators in the spin-drone representation.[15,16] More precisely, we are using the following ansatz, which our further calculations will be relied on:

$$\hat{S}^z_{5/2} \approx 5\hat{S}^z_{1/2}, \tag{1}$$

where the $\frac{5}{2}$-spin states, $|\frac{5}{2},+\frac{5}{2}\rangle$, and $|\frac{5}{2},+\frac{3}{2}\rangle$, which are only relevant states in describing low-temperature magnon dynamics, can be drone mapped as spin-up and spin-down states of $S=\frac{1}{2}$, respectively. By this approximation, all the second and higher order spin-flip processes, related to magnon-magnon interactions, are neglected. In the temperature region below the Néel temperature, due to the condition $1/zS \ll 1$, where z (=18) is the number of spins interacting with any given spin of the absolute value $S=\frac{5}{2}$ (cf. Fig. 1), we do not need to perform calculations beyond the framework of linear spin wave theory and the introduced assumption is expected to be quite suitable.[17] A similar assumption was applied by Spencer[16] for the case of spin $S=1$. It was furthermore shown[18,19] that such an approach becomes highly favorable in weakly coupled systems, such as in our case (weak magnon- and magnon-phonon interaction).

Applying the ansatz [Eq. (1)], we can obtain the following relations for the modified spin-drone representation, on the lattice sites i,j belonging to two different sublattices:

$$\hat{S}^+_i = \sqrt{5}\hat{c}^\dagger_i\hat{\varphi}_i, \quad \hat{S}^+_j = \sqrt{5}\hat{\varphi}_j\hat{c}_j,$$

$$\hat{S}_i^z = 5\hat{c}_i^\dagger \hat{c}_i - \tfrac{5}{2}, \quad \hat{S}_j^z = \tfrac{5}{2} - 5\hat{c}_j^\dagger \hat{c}_j,$$

$$\hat{\varphi}_i = \hat{d}_i^\dagger + \hat{d}_i, \quad \hat{\varphi}_j = \hat{d}_j^\dagger + \hat{d}_j, \tag{2}$$

where $\hat{c}$ and $\hat{d}$ are fermion anticommuting operators: $\{\hat{c}_i, \hat{c}_j^\dagger\} = \delta_{ij}$, $\{\hat{d}_i, \hat{d}_j^\dagger\} = \delta_{ij}$.

The Fourier transformation into reciprocal space is given by

$$\hat{c}_i^\dagger = \frac{1}{\sqrt{N}} \sum_{\mathbf{q}} e^{i\mathbf{q}\cdot\mathbf{l}_i} \hat{c}_{1\mathbf{q}}^\dagger, \quad \hat{\varphi}_i = \frac{1}{\sqrt{N}} \sum_{\mathbf{q}} e^{i\mathbf{q}\cdot\mathbf{l}_i} \hat{\varphi}_{1\mathbf{q}},$$

$$\hat{c}_j^\dagger = \frac{1}{\sqrt{N}} \sum_{\mathbf{q}} e^{-i\mathbf{q}\cdot\mathbf{l}_j} \hat{c}_{2\mathbf{q}}^\dagger, \quad \hat{\varphi}_j = \frac{1}{\sqrt{N}} \sum_{\mathbf{q}} e^{-i\mathbf{q}\cdot\mathbf{l}_j} \hat{\varphi}_{2\mathbf{q}}, \tag{3}$$

where N is the number of sites in each sublattice (equal to number of unit cells).

We shall use the slightly modified Heisenberg Hamiltonian for $S = \frac{5}{2}$ which includes the exchange interaction between the nearest neighbors (nn), J_1, next-nearest neighbors (nnn), J_2, and small magnetic anisotropy term in addition,

$$\hat{H} = \sum_{\langle i,i' \rangle}^{nn} \hat{\mathbf{S}}_i \hat{J}_1 \hat{\mathbf{S}}_{i'} + \sum_{\langle j,j' \rangle}^{nn} \hat{\mathbf{S}}_j \hat{J}_1 \hat{\mathbf{S}}_{j'} + \sum_{\langle i,j \rangle}^{nn} \hat{\mathbf{S}}_i \hat{J}_1 \hat{\mathbf{S}}_j + \sum_{\langle i,j \rangle}^{nnn} \hat{\mathbf{S}}_i \hat{J}_2 \hat{\mathbf{S}}_j, \tag{4}$$

$$\hat{J}_i = J_i \times \begin{pmatrix} 1 & 0 & 0 \\ 0 & 1 & 0 \\ 0 & 0 & 1 + g_i \end{pmatrix}, \quad i \in \{1,2\}, \quad g_1 \approx g_2 \equiv g. \tag{5}$$

According to Fig. 1, $\langle i,i' \rangle$ and $\langle j,j \rangle'$ indices correspond to spin-up and spin-down sublattices, respectively, while g denotes the pseudodipolar anisotropy contribution to the exchange constants.[20,21] Due to the fact that $g_{1,2} \ll 1$, the simplification we made, $g_1 \approx g_2 \equiv g$, is not seriously limiting our further conclusions.

By means of standard implementation of the spin-drone representation in the mean field approximation, one can obtain the sublattice magnetizations,[22,23]

$$\mathcal{M}_{1,2}(T) = \langle \hat{S}_{1,2}^z \rangle_T = 5(-1)^{1,2} \left\langle \frac{1}{2} + \hat{c}_{1,2} \hat{c}_{1,2}^\dagger \right\rangle_T$$

$$= \frac{5}{2} \tanh\left(\frac{5}{2} \frac{1}{k_B T} \mathcal{M}_{1,2}(T)[A(\mathbf{0}) - B(\mathbf{0})] \right), \tag{6}$$

where $A(\mathbf{q})$ and $B(\mathbf{q})$ are the off-diagonal and diagonal $\mathbf{q}$-space exchange interactions, respectively,

$$A(\mathbf{q}) = 2J_1 \left(\cos\frac{x+y}{2} + \cos\frac{y+z}{2} + \cos\frac{z+x}{2} \right)$$

$$+ 2J_2(\cos x + \cos y + \cos z),$$

$$B(\mathbf{q}) = 2J_1 \left(\cos\frac{x-y}{2} + \cos\frac{y-z}{2} + \cos\frac{z-x}{2} \right), \tag{7}$$

with

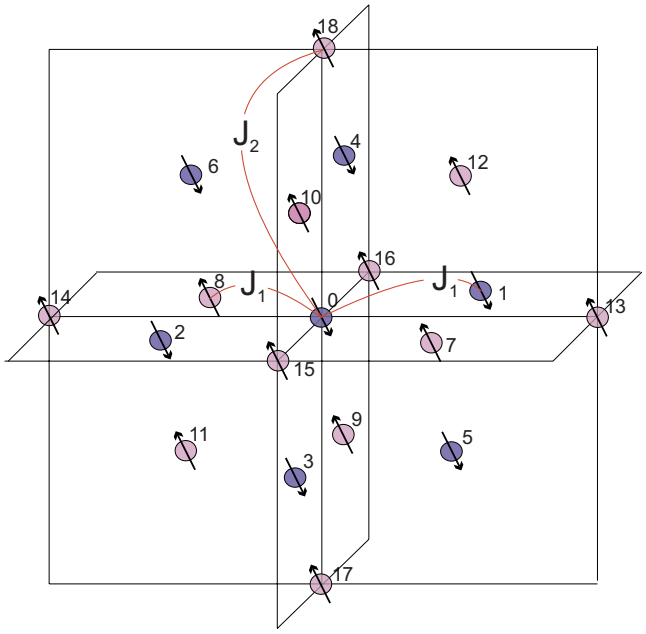

FIG. 1. (Color online) The fcc lattice of α-MnSe in the antiferromagnetic phase with an arbitrary spin direction. Here, 1–12 are the labels for the nearest-neighbor ions and 13–18 are respective labels for the next-nearest neighbors.

$$x = q_x a, \quad y = q_y a, \quad z = q_z a, \tag{8}$$

where $a = 5.464$ Å, Ref. 24.

The Néel temperature is determined by solving Eq. (6) with respect to T when the sublattice magnetization becomes finite. Similarly, by converting $A(\mathbf{0})$ into $-A(\mathbf{0})$, we come up with θ temperature, which is an analog to the Curie-Weiss temperature when, hypothetically, all the spins in the system are turned to be ferromagnetically aligned. Then, one can easily obtain that

$$k_B T_N = \frac{75}{2}(1+g)J_2, \tag{9}$$

$$-k_B \theta = \frac{75}{2}(1+g)(J_2 + 2J_1). \tag{10}$$

Formulas (9) and (10) are in good agreement with the respective ones obtained by use of the Holstein-Primakoff representation for $\frac{5}{2}$ spins on manganese atoms in Ref. 25. This is the trump for the justification of our starting approximation [Eq. (1)].

Relying on the magnetic susceptibility measurements carried out in Ref. 7 and on the assumption that there are no structural changes below the magnetic phase transition temperature, one can come up with $\theta = -335$ K, $T_N = 130$ K, and the exchange interaction parameters, $J_1 = 1.94$ cm^{-1} and $J_2 = 2.46$ cm^{-1} as well. Respecting the fact that the AF exchange interaction J_2 stabilizes the system in some kind of AF ordered state, contrary to the AF interaction J_1 that

frustrates it, and bearing in mind the calculated ratio, $J_2/J_1=1.27>1/2$, the stability of the suggested AF ordering is maintained.[25,26]

After justifiably omitting all magnon-magnon interaction terms, the magnon dispersion relation can be calculated in the order of $(1/z)^1$ from the following transversal magnon propagator:[22,23]

$$\mathcal{T}^{(1)}_{mn}(\mathbf{k},\tau)=\langle\hat{\theta}\hat{S}^{-}_{m\mathbf{k}}(\tau)\hat{S}^{+}_{n\mathbf{k}}(0)\rangle, \tag{11}$$

where m,n are the sublattice indices (1 or 2) and $\hat{\theta}$ is the time ordering operator. Upon solving the corresponding Dyson's equation, the expression for this propagator in the imaginary time representation, $\mathcal{T}^{(1)}_{m,n}(\mathbf{k},i\omega)$, is given by

$$\hat{\mathcal{T}}^{(1)}(\mathbf{k},i\omega)=\frac{2\mathcal{M}}{E^2_{\mathbf{k}}+\omega^2}\times\begin{pmatrix}\Xi^{+}(\mathbf{k},i\omega) & A(\mathbf{k})\mathcal{M}\\ A(\mathbf{k})\mathcal{M} & \Xi^{-}(\mathbf{k},i\omega)\end{pmatrix}, \tag{12}$$

where

$$\Xi^{\pm}(\mathbf{k},i\omega)=\pm i\omega+(1+g)[A(\mathbf{0})+B(\mathbf{0})]\mathcal{M}-B(\mathbf{k}),$$
$$\mathcal{M}=|\mathcal{M}_{1,2}|, \tag{13}$$

and the magnon dispersion relation reads

$$E_{\mathbf{k}}(T)=\mathcal{M}(T)\sqrt{\{(1+g)[A(\mathbf{0})+B(\mathbf{0})]-B(\mathbf{k})\}^2-A^2(\mathbf{k})}. \tag{14}$$

The same dispersion relation can be found in Ref. 17. This is additional factor in favor of our starting ansatz [Eq. (1)].

Diagonalizing $\hat{\mathcal{T}}^{(1)}(\mathbf{k},i\omega)$ by means of the Bogoliubov's canonical transformation,

$$\tilde{T}(\mathbf{k},i\omega)=\mathcal{S}^{\dagger}(\mathbf{k})\hat{\mathcal{T}}^{(1)}(\mathbf{k},i\omega)\mathcal{S}(\mathbf{k}), \tag{15}$$

we come up with

$$\tilde{T}(\mathbf{k},i\omega)=2\mathcal{M}\begin{pmatrix}\dfrac{1}{E_{\mathbf{k}}-i\omega} & 0\\ 0 & \dfrac{1}{E_{\mathbf{k}}-i\omega}\end{pmatrix},$$

$$\mathcal{S}(\mathbf{k})=\begin{pmatrix}\alpha_{\mathbf{k}} & -\beta_{\mathbf{k}}\\ -\beta_{\mathbf{k}} & \alpha_{\mathbf{k}}\end{pmatrix}, \tag{16}$$

$$\alpha^2_{\mathbf{k}}=\frac{1}{2}\left\{\left[1-\left(\frac{A(\mathbf{k})}{(1+g)[A(\mathbf{0})+B(\mathbf{0})]-B(\mathbf{k})}\right)^2\right]^{-1/2}+1\right\},$$

$$\alpha^2_{\mathbf{k}}-\beta^2_{\mathbf{k}}=1. \tag{17}$$

Unlike the transversal magnon propagator $\tilde{T}(\mathbf{k},i\omega)$, the longitudinal one does not have terms of the order of $(1/z)^1$. Even if one wanted to take into account longitudinal spin-fluctuation phenomena in higher orders $(1/z)^{n>1}$, such contributions would be irrelevant because of the $\delta_{\omega 0}$ factor involved in the longitudinal propagator, whereas we are interested in the finite frequencies optically active phonon modes.[22]

III. SPIN-PHONON INTERACTION IN α-MnSe

This section gives details of the spin system influence upon the lattice dynamics in the ordered phase of α-MnSe. Our calculations are carried out for the extended form of the Heisenberg Hamiltonian (4) that includes spin-phonon interaction terms in a standard way by expanding the exchange integrals in the powers of ionic displacements.[12,13] The spin-phonon interaction terms in the extended Heisenberg Hamiltonian are easily obtained by taking into account only the first derivative with respect to atomic displacements of the J_2 exchange integral. This is a consequence of the evident fact that, for the infrared active phonon modes[7] and the suggested magnetic ordering, all the (nn) contributions exactly cancel each other (every Mn ion is surrounded by the equal number of spin-up and spin-down ions). Thus, the spin-phonon interaction in α-MnSe with the suggested AF ordering is driven only by the last term in the modified Heisenberg Hamiltonian (4). The expansion of that term in ionic displacements gives

$$\hat{H}^{sp\text{-}ph}=\sum_{\langle i,j\rangle}^{nnn}\hat{\mathbf{S}}_i\{(\mathbf{x}_i-\mathbf{x}_j)\cdot\{\hat{\nabla}_{\mathbf{R}_i-\mathbf{R}_j}\hat{J}_2(\mathbf{R}_i-\mathbf{R}_j)\}|_{\mathbf{0}}\}\hat{\mathbf{S}}_j, \tag{18}$$

where $\mathbf{l}_i$ and $\mathbf{l}_j$ enumerate equilibrium ionic position in up and down spin sublattices, and

$$\mathbf{R}_{i,j}=\mathbf{l}_{i,j}+\mathbf{x}_{i,j}, \tag{19}$$

$$\hat{J}_2(\mathbf{l}_i+\mathbf{x}_i-\mathbf{l}_j-\mathbf{x}_j)\approx\hat{J}_2(\mathbf{l}_i-\mathbf{l}_j)+(\mathbf{x}_i-\mathbf{x}_j)\cdot\{\hat{\nabla}_{\mathbf{R}_i-\mathbf{R}_j}\hat{J}_2(\mathbf{R}_i-\mathbf{R}_j)\}|_{\mathbf{0}},$$

$$\hat{J}_2(\mathbf{l}_i-\mathbf{l}_j)\equiv\hat{J}_2. \tag{20}$$

The expansion of displacements $\mathbf{x}_i$ from their equilibrium position $\mathbf{l}_i$ in normal modes is given by

$$\mathbf{x}_i=\sqrt{\frac{\hbar}{2NM_i}}\sum_{\mathbf{q},\lambda}\frac{1}{\sqrt{\Omega_{\mathbf{q},\lambda}}}\mathbf{w}(\mathbf{q},\lambda)e^{i\mathbf{q}\cdot\mathbf{l}_i}(\hat{b}_{\mathbf{q},\lambda}+\hat{b}^{\dagger}_{-\mathbf{q},\lambda}). \tag{21}$$

Here, the phonon field operator is given by $\hat{\Phi}_{\mathbf{q},\lambda}=\hat{b}_{\mathbf{q},\lambda}+\hat{b}^{\dagger}_{-\mathbf{q},\lambda}$, $\Omega_{\mathbf{q},\lambda}$ is the normal mode frequency with wave vector $\mathbf{q}$ and branch index λ (LO, TO, TA,…), $\mathbf{w}(\mathbf{q},\lambda)$ is the polarization vector of the normal mode, $\hat{b}^{\dagger}_{\mathbf{q},\lambda}$ and $\hat{b}_{\mathbf{q},\lambda}$ are phonon creation and annihilation operators, N is the number of unit cells in the crystal, and M_i stands for the ionic mass.

Equations (18) and (21) give for the effective spin-phonon Hamiltonian,

$$\hat{H}^{sp\text{-}ph}=\sum_{\langle i,j\rangle}^{nnn}\sum_{\mathbf{q},\lambda}\hat{\Phi}_{\mathbf{q},\lambda}\hat{\mathbf{S}}_i\hat{\mathcal{K}}(\mathbf{l}_i,\mathbf{l}_j,\mathbf{q},\lambda)\hat{\mathbf{S}}_j, \tag{22}$$

with

$$\hat{\mathcal{K}}(\mathbf{l}_i,\mathbf{l}_j,\mathbf{q},\lambda)=\sqrt{\frac{\hbar}{2NM\Omega_{\mathbf{q},\lambda}}}(e^{i\mathbf{q}\cdot\mathbf{l}_i}-e^{i\mathbf{q}\cdot\mathbf{l}_j})\times\{[\mathbf{w}(\mathbf{q},\lambda)\cdot\hat{\nabla}_{\mathbf{R}_i-\mathbf{R}_j}]\hat{J}_2(\mathbf{R}_i-\mathbf{R}_j)\}|_{\mathbf{0}}. \tag{23}$$

Accordingly, for the infrared active phonon mode ($\mathbf{q}\approx 0$, $\Omega_{\mathbf{q},\lambda}\equiv\Omega$), we can write

TABLE I. The phonon-phonon and magnon-phonon fitting parameters of the LO phonon mode Ω_{01} and the one combinational two-phonon mode Ω_{02}. .

Phonon frequency (cm^{-1})	Phonon-phonon parameter (cm^{-1})	Magnon-phonon parameter (cm^{-1})
$\Omega_{01}=230.40$	$C_1=0.81$	$K_1=2.37$
$\Omega_{02}=224.60$	$C_2=1.78$	$K_2=2.33$

$$\mathcal{K}^{\mu\nu}(\mathbf{l}_i,\mathbf{l}_j,\mathbf{q},\lambda) \approx i\sqrt{\frac{\hbar}{2NM\Omega}}\mathbf{q}\cdot(\mathbf{l}_i-\mathbf{l}_j) \times \{[\mathbf{w}(\mathbf{q})\cdot\hat{\nabla}_{\mathbf{R}_i-\mathbf{R}_j}]J_2^{\mu\nu}(\mathbf{R}_i-\mathbf{R}_j)\}|_{\mathbf{0}},$$

which after the Fourier transformation and in the limit of small phonon wave vectors becomes

$$\mathcal{K}^{\mu\nu}(\mathbf{Q},\mathbf{q}\approx 0) \sim i\left(\mathbf{q}\cdot\frac{\partial}{\partial\mathbf{Q}}\right)\{[\mathbf{w}(\mathbf{q})\cdot\mathbf{Q}]J_2^{\mu\nu}(\mathbf{Q})\}. \quad (24)$$

Finally, we are making an ultimate simplification which is expected to be appropriate for the optical infrared phonons we are dealing with in the present work. Instead of the **Q**-dependent spin-phonon interaction tensor, the constant diagonal tensor describing the magnon-phonon interaction is thus introduced as

$$\frac{1}{2}|\hat{\mathcal{K}}(\mathbf{Q},\mathbf{q}\approx 0)| \equiv \begin{pmatrix} K & 0 & 0 \\ 0 & K & 0 \\ 0 & 0 & (1+g)K \end{pmatrix}. \quad (25)$$

Magnon-phonon interaction constant K is expected to be much smaller than the characteristic frequency of optical modes in crystals (cf. Table I in the present work). The approximation [Eq. (25)] provides the simplest possible way of connecting the theory with the experimental data. This is allowed by the fact that Eq. (24) possesses very small q factor which smoothes the **Q** dependence of the whole expression.

The diagrammatic expression for the magnon-phonon interaction is given in Fig. 2, where the shaded circle represents the magnon-phonon interaction vertex with the additional vertex condition $m\neq n_1$, caused by the fact that the

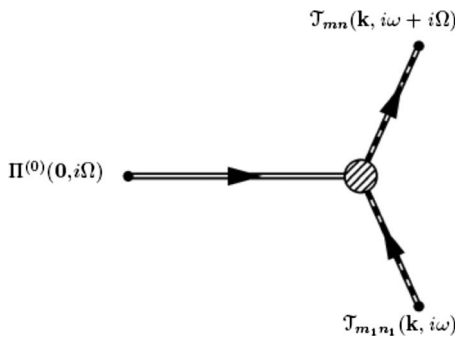

FIG. 2. The magnon-phonon interaction diagram.

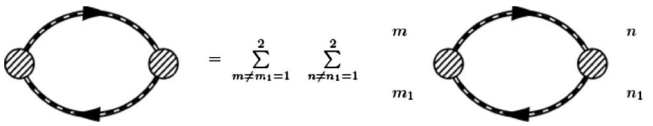

FIG. 3. The self-energy represented by four intersublattice pair-bubble parts.

magnon-phonon interaction has been obtained through the expansion of exchange interaction J_2 connecting different sublattices.

Renormalizing the bare optical phonon propagator $\Pi^{(0)}(\mathbf{q}\approx\mathbf{0},i\Omega)$ by the magnon-phonon interaction terms, we come up with the following Dyson's equation:

$$\Pi(\mathbf{0},i\Omega) = \frac{1}{\frac{1}{\Pi^{(0)}(\mathbf{0},i\Omega)} - \Sigma(\mathbf{0},i\Omega)}, \quad (26)$$

with the self-energy $\Sigma(0,i\Omega)$ represented by four intersublattice pair-bubble parts[27] in the diagram given in Fig. 3.

After straightforward, but analytically tedious manipulations, one can show that the explicit expression for the phonon self-energy operator is

$$\Sigma(\mathbf{0},i\Omega) = \frac{4K^2\mathcal{M}^2}{\beta N}\sum_{\mathbf{k}}\sum_{n=-\infty}^{n=+\infty}(\alpha_{\mathbf{k}}^2+\beta_{\mathbf{k}}^2)^2 \times\left(\frac{1}{i\omega_n+E_{\mathbf{k}}}\frac{1}{-i\omega_n-i\Omega+E_{\mathbf{k}}} + \frac{1}{-i\omega_n+E_{\mathbf{k}}}\frac{1}{i\omega_n+i\Omega+E_{\mathbf{k}}}\right) + 4\alpha_{\mathbf{k}}^2\beta_{\mathbf{k}}^2\left(\frac{1}{i\omega_n+E_{\mathbf{k}}}\frac{1}{i\omega_n+i\Omega+E_{\mathbf{k}}} + \frac{1}{-i\omega_n+E_{\mathbf{k}}}\frac{1}{-i\omega_n-i\Omega+E_{\mathbf{k}}}\right). \quad (27)$$

Performing the Matsubara summation over the imaginary boson frequencies by converting the sum to a contour integral[27] yields the result,

$$\Sigma[\mathbf{0},\Omega(T)] = -16K^2\mathcal{M}^2(T)\frac{1}{N}\sum_{\mathbf{k}}(\alpha_{\mathbf{k}}^2+\beta_{\mathbf{k}}^2)^2\coth\left(\frac{E_{\mathbf{k}}(T)}{2k_BT}\right) \times\frac{E_{\mathbf{k}}(T)}{4E_{\mathbf{k}}^2(T)+[i\Omega(T)]^2+i\eta}, \quad (28)$$

where $\Sigma_{\mathbf{k}}$ represents summation over all the magnon degrees of freedom. Thus, we obtain the renormalized phonon frequency as

$$\Omega_R(T) = \Omega(T) + \Delta\Omega(T). \quad (29)$$

Here,

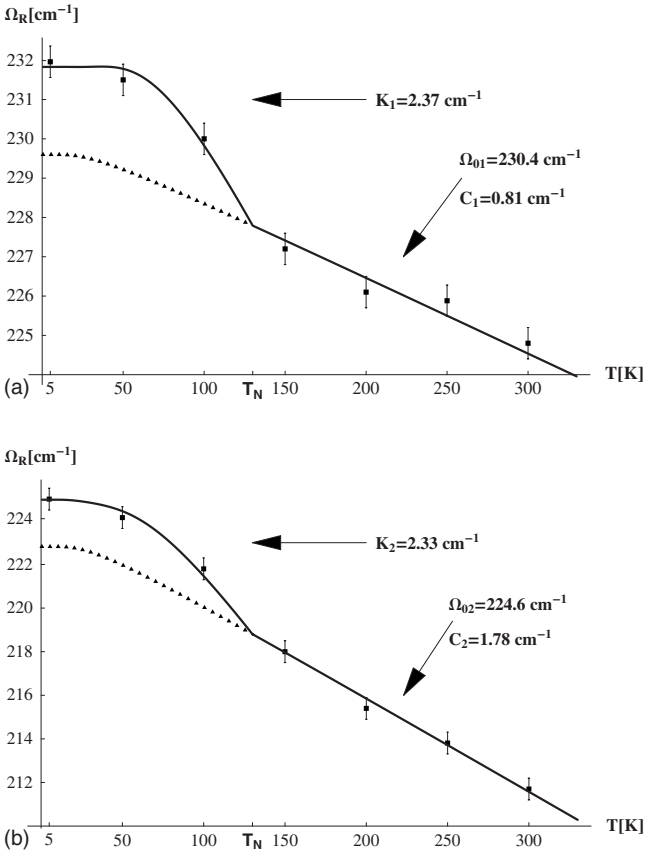

FIG. 4. (a) The visual survey of longitudinal optical phonon mode Ω_{01} and (b) combinational two-phonon mode Ω_{02} as a function of temperature. Squares with the error bars are the experimental results (Ref. 7), the full lines are our theoretical curves, whereas the triangles represent the residue of phonon hardening due to the phonon-phonon anharmonicity.

$$\Omega(T) = \Omega_0 - C\left(1 + \frac{2}{e^{(\hbar\Omega_0/2k_BT)} - 1}\right) \tag{30}$$

is the renormalized bare phonon frequency Ω_0 on the basis of the standard Balkanski's procedure which takes into account phonon-phonon interaction terms,[28] C is the phonon-phonon interaction strength, and

$$\Delta\Omega(T) = \mathrm{Re}\{\Sigma[\mathbf{0}, \Omega(T)]\} \tag{31}$$

is presently calculated renormalization due to the magnon-phonon interaction. Note, just for completeness, that the renormalized optical phonon has the infinitesimally small damping up to the $i\eta$ factor.

IV. RESULTS AND DISCUSSION

Let us proceed further with the comparison of theoretical model presented in previous sections with the recent infrared reflectivity measurements in α-MnSe.[7] These experimental data clearly point to the additional phonon frequency hardening for temperatures below the AF transition temperature at 130 K (cf. Fig. 4). There are two basic fitting parameters: C and K which, as we already mentioned, represent the phonon-phonon and magnon-phonon interaction strength constants, respectively. In addition, we have introduced the small anisotropy parameter g. It occurs that a slight extension of the the Heisenberg Hamiltonian (4), in order to include an anisotropy, is particularly relevant for getting quantitative agreement with the experiments. We have found that the anisotropy parameter should be $g \gtrsim 10^{-2}$, if one wanted to obtain suitable order of phonon hardening. This is in accordance with a common wisdom regarding the coupling of the magnetic system with the crystal lattice through the magnetic anisotropy energy. Using the one-magnon Raman excitation observed at $\approx 18\ cm^{-1}$ in α-MnSe (Ref. 8) enables us to fix the true value of the anisotropy parameter, i.e., $g \approx 3 \times 10^{-2}$.

Note here that the anisotropies induced in the vibrational spectrum of transition-metal monoxide MnO (closely related to α-MnSe), solely by AF ordering, were investigated theoretically on the basis of accurate *ab initio* (mostly density-functional) and semiempirical calculations.[29] These authors found the anisotropy important both in the $\mathbf{q}=0$ optic phonon frequencies and in the dynamical charge tensor. They revealed that manganese monoxide MnO below T_N, despite having a cubic ionic arrangement and a practically cubic electron density, has a noncubic electronic response with strong enhancement of the weak anisotropy influenced by low-symmetry perturbations.

At last, we performed fitting the recently measured infrared phonon frequencies in the temperature range of 5–300 K (one LO phonon mode and one combinational two-phonon mode) using the microscopically calculated expression for the renormalized phonon frequencies $\Omega_R(T)$ [Eq. (29)]. Our results are presented in Fig. 4 and Table I. Almost perfect agreement with the experimental results, as well as the fitting parameters which have clear physical meaning, makes this straightforward approach very promising. One can infer from Table I that the fitting parameters take quite reasonable values. Thus, we have right to expect that the fitting function could also be useful for predicting eventual phonon softening in the region of phonon frequencies of the order of 100 cm^{-1} and less.

In conclusion, we have developed a microscopic approach for the renormalization of the phonon spectra due to the spin-phonon interaction terms. By means of detailed comparison between theory and experiment for the infrared optical phonon hardening in the antiferromagnetic phase of α-MnSe, the phonon-phonon and spin-phonon interaction parameters are estimated for this compound, as well as the exchange interactions for the nearest and next-nearest neighbors. We have found that the inclusion of the anisotropy has been essential for obtaining quantitative agreement with the experimental results.

ACKNOWLEDGMENTS

This paper has been completed, thanks to financial support of the Serbian Ministry of Science under the Contracts No. 141047 and No 141039. One of us (D.M.D.) is pleased to thank R. Gajić, M. Damnjanović, A. Beltaos, N. Paunović, and G. Kodžo for their great help.

*djokic@phy.bg.ac.yu

[1] R. Loudon, Adv. Phys. **17**, 243 (1968).
[2] E. Anda, J. Phys. C **9**, 1075 (1976).
[3] K. Wakamura and T. Arai, Phase Transitions **27**, 129 (1990).
[4] X. B. Wang, J. X. Li, Q. Jiang, Z. H. Zhang, and D. C. Tian, Phys. Rev. B **50**, 7056 (1994).
[5] D. U. Saenger, Phys. Rev. B **52**, 1025 (1995).
[6] A. Wurger, Phys. Rev. B **57**, 347 (1998).
[7] Z. V. Popović and A. Milutinović, Phys. Rev. B **73**, 155203 (2006).
[8] A. Milutinović, N. Tomić, S. Dević, P. Milutinović, and Z. V. Popović, Phys. Rev. B **66**, 012302 (2002).
[9] D. J. Lockwood and M. G. Cottam, J. Appl. Phys. **64**, 5876 (1988).
[10] D. J. Lockwood, Low Temp. Phys. **28**, 505 (2002).
[11] W. Baltensperger and J. S. Helman, Helv. Phys. Acta **41**, 668 (1968).
[12] G. Meissner, Z. Phys. **237**, 272 (1970).
[13] F. Vukajlović, H. Konwent, and N. M. Plakida, Theor. Math. Phys. **19**, 115 (1974).
[14] A. B. Migdal, Sov. Phys. JETP **34**, 996 (1958).
[15] D. C. Mattis, *Theory of Magnetism* (Harper, New York, 1965).
[16] H. J. Spencer, Phys. Rev. **167**, 430 (1968).
[17] R. J. Elliott and M. F. Thorpe, J. Phys. C **2**, 1630 (1969).
[18] B. J. McKenzie and G. E. Stedman, J. Phys. A **9**, 187 (1976).
[19] S. E. Barnes, J. Phys. C **5**, L178 (1972).
[20] S. Maekawa, T. Tohyama, S. E. Barnes, S. Ishihara, W. Koshibae, and G. Khaliullin, *Physics of Transition Metal Oxides* (Springer-Verlag, Berlin, 2004).
[21] K. Yosida, J. Appl. Phys. **39**, 511 (1968).
[22] M. G. Cottam and R. B. Stinchcombe, J. Phys. C **3**, 2283 (1970).
[23] M. G. Cottam and R. B. Stinchcombe, J. Phys. C **3**, 2305 (1970).
[24] T. Ito, K. Ito, and M. Oka, Jpn. J. Appl. Phys. **17**, 371 (1978).
[25] R. H. Swendsen, Phys. Rev. B **13**, 3912 (1976).
[26] M. C. Moron, J. Phys.: Condens. Matter **8**, 11141 (1996).
[27] R. D. Mattuck, *A Guide to Feynman Diagrams in the Many-Body Problem* (Dover, New York, 1992).
[28] R. F. Wallis and M. Balkanski, *Many-Body Aspects of Solid State Spectroscopy* (North-Holland, Amsterdam, 1986).
[29] S. Massidda, M. Posternak, A. Baldereschi, and R. Resta, Phys. Rev. Lett. **82**, 430 (1999).